Scalable PCG Algorithms for Numerical Upscaling of Voxel Structures

Yavor Vutov

Abstract Numerical homogenization is applied for upscaling of the linear elasticity tensor of strongly heterogeneous microstructures. Rannacher-Turek finite elements are used for the discretization. The scalability of two parallel PCG solvers is studied. Both are based on displacement decomposition. The first one uses modified incomplete Cholesky factorization MIC(0) and the other – algebraic multigrid. The numerical homogenization scheme is based on the assumption of a periodic microstructure. This implies the use of periodic boundary conditions on the reference volume element. Numerical upscaling results are shown. The test problem represents a trabecular bone tissue. The voxel microstructure of the bone is extracted from a high resolution computer tomography image.

1 Introduction

Many materials, such as human bone and composite materials have a complex microstructure. The macro level material properties strongly depend on their microstructure. The overall mechanical responses can be described using multilevel techniques that are built upon basic conservation principles at the micro level.

In this work we consider a human trabecular bone tissue. Its voxel representation obtained from a micro computer tomography images is used to formulate the problem. Here, the computational domain is a strongly heterogeneous composition of solid and fluid phases. Our goal is to obtain upscaled material properties of trabecular bone tissue. As a first step, in this paper, the mechanical response of the solid phase only, is taken into account. To this purpose a fictitious domain approach is used. The isotropic linear elasticity model considered here is a brick in the development of a toolkit for μFE simulation of the bone micro-structure.

Yavor Vutov
Institute for Parallel Processing - BAS, 25A G. Bonchev str., 1113 Sofia, Bulgaria,
e-mail: yavor@parallel.bas.bg

The 3D nature of the problems leads after a discretization to a very large linear systems. This, in turn, leaves no other approach to solve them but application of parallel computers. The large size also implies the use of iterative solvers. The preconditioned conjugate gradient (PCG) method is known to be the best solution tool for large systems of linear equations with symmetric and positive definite sparse matrices [6]. It is also know that the PCG method converges for semidefinite matrices in the orthogonal to the kernel subspace. The used preconditioning technique is crucial for the PCG performance. In this work two parallel preconditioners are applied for the solution of the arising linear system. The first one uses incomplete factorization, the other – algebraic multigrid [1].

This paper is organized as follows. The applied numerical homogenization scheme is described in Section 2. In Section 3 we introduce the used preconditioning methods. Results from numerical experiments are presented in the last section.

2 Homogenization Technique

Let Ω be a parallelepipedal domain representing our reference volume element (RVE) and $\mathbf{u} = (u_1, u_2, u_3)$ be the displacements vector in Ω. Here, components of the small strain tensor are:

$$\varepsilon_{ij}(\mathbf{u}(\mathbf{x})) = \frac{1}{2}\left(\frac{\partial u_i(\mathbf{x})}{\partial x_j} + \frac{\partial u_j(\mathbf{x})}{\partial x_i}\right) \tag{1}$$

We assume that Hooke's law holds:

$$\begin{bmatrix}\sigma_{11}\\ \sigma_{22}\\ \sigma_{33}\\ \sigma_{23}\\ \sigma_{13}\\ \sigma_{12}\end{bmatrix} = \begin{bmatrix} c_{1111} & c_{1122} & c_{1133} & c_{1123} & c_{1113} & c_{1112}\\ c_{2211} & c_{2222} & c_{2233} & c_{2223} & c_{2213} & c_{2212}\\ c_{3311} & c_{3322} & c_{3333} & c_{3323} & c_{3313} & c_{3312}\\ c_{2311} & c_{2322} & c_{2333} & c_{2323} & c_{2313} & c_{2312}\\ c_{1311} & c_{1322} & c_{1333} & c_{1323} & c_{1313} & c_{1312}\\ c_{1211} & c_{1222} & c_{1233} & c_{1223} & c_{1213} & c_{1212}\end{bmatrix} \begin{bmatrix}\varepsilon_{11}\\ \varepsilon_{22}\\ \varepsilon_{33}\\ 2\varepsilon_{23}\\ 2\varepsilon_{13}\\ 2\varepsilon_{12}\end{bmatrix}. \tag{2}$$

Here, tensor c is called the stiffness tensor, while σ is the stress tensor.

The symmetric 6×6 matrix C is called the stiffness matrix. For an isotropic material C has only two independent degrees of freedom. For orthotropic materials (materials containing three orthogonal planes of symmetry), matrix C has nine independent degrees of freedom: three Young's moduli E_1, E_2, E_3, three Poisson's ratios $\nu_{12}, \nu_{23}, \nu_{31}$ and three shear moduli $\mu_{12}, \mu_{23}, \mu_{31}$. The stiffness matrix for orthotropic materials takes the following form:

$$C = \delta \begin{bmatrix} \frac{1-\nu_{23}\nu_{32}}{E_1} & \frac{\nu_{12}+\nu_{31}\nu_{23}}{E_1} & \frac{\nu_{31}+\nu_{21}\nu_{32}}{E_1} & & & \\ \frac{\nu_{12}+\nu_{13}\nu_{32}}{E_2} & \frac{1-\nu_{31}\nu_{13}}{E_2} & \frac{\nu_{32}+\nu_{31}\nu_{12}}{E_2} & & & \\ \frac{\nu_{13}+\nu_{12}\nu_{23}}{E_3} & \frac{\nu_{23}+\nu_{13}\nu_{21}}{E_3} & \frac{1-\nu_{12}\nu_{21}}{E_3} & & & \\ & & & \frac{\mu_{23}}{\delta} & & \\ & & & & \frac{\mu_{31}}{\delta} & \\ & & & & & \frac{\mu_{12}}{\delta} \end{bmatrix}, \tag{3}$$

where

$$\delta = 1-\nu_{12}\nu_{21}-\nu_{13}\nu_{31}-\nu_{23}\nu_{32}-2\nu_{12}\nu_{23}\nu_{31},$$
$$\frac{\nu_{12}}{E_1}=\frac{\nu_{21}}{E_2}, \qquad \frac{\nu_{23}}{E_2}=\frac{\nu_{32}}{E_3}, \qquad \frac{\nu_{31}}{E_3}=\frac{\nu_{13}}{E_1}.$$

The goal of our study was to obtain homogenized material properties of the trabecular bone tissue. In other words – to find the stiffness tensor of a homogeneous material which would have the same macro-level properties as our RVE. Our approach follows the numerical upscaling method from [10] (see also [9]). The homogenization scheme requires finding Ω-periodic functions $\xi^{kl} = (\xi_1^{kl}, \xi_2^{kl}, \xi_3^{kl})$, k, $l = 1,2,3$, satisfying the following problem in a week formulation:

$$\int_\Omega \left(c_{ijpq}(x) \frac{\partial \xi_p^{kl}}{\partial x_q} \right) \frac{\partial \phi_i}{\partial x_j} d\Omega = \int_\Omega c_{ijkl}(x) \frac{\partial \phi_i}{\partial x_j} d\Omega, \tag{4}$$

for an arbitrary Ω-periodic variational function $\phi \in H^1(\Omega)$. After computing the characteristic displacements ξ^{kl}, from (4) we can compute the homogenized elasticity tensor c^H using the following formula:

$$c_{ijkl}^H = \frac{1}{|\Omega|} \int_\Omega \left(c_{ijkl}(x) - c_{ijpq}(x) \frac{\partial \xi_p^{kl}}{\partial x_q} \right) d\Omega. \tag{5}$$

Due to the symmetry of the stiffness tensor c, we have the relation $\xi^{kl} = \xi^{lk}$. Therefore the solution of only six problems (4) is required to obtain the homogenized stiffness tensor.

The periodicity of the solution implies the use of periodic boundary conditions. Rotated trilinear (Rannacher-Turek) finite elements [12] are used for the numerical solution of (4). This choice is motivated by the additional stability of the nonconforming finite element discretization in the case of strongly heterogeneous materials [4]. Construction of a robust non-conforming finite element method is generally based on application of mixed formulation leading to a saddle-point system. By the choice of non continuous finite elements for the dual (pressure) variable, it can be eliminated at the (macro)element level. As a result we obtain a symmetric positive

semi-definite finite element system in primal (displacements) variables. We utilize this approach, which is referred as the *reduced and selective integration* (RSI) [2].

3 Preconditioning algorithms

Both of the considered preconditioners are based on the isotropic variant of the displacement decomposition (DD)[11]. We write the DD auxiliary matrix in the form

$$C_{DD} = \begin{bmatrix} A & & \\ & A & \\ & & A \end{bmatrix} \tag{6}$$

where A is the stiffness matrix corresponding to the bilinear form

$$a(u^h, v^h) = \sum_{e \in \Omega^h} \int_e E \left(\sum_{i=1}^{3} \frac{\partial u^h}{\partial x_i} \frac{\partial v^h}{\partial x_i} \right) de. \tag{7}$$

Such approach is motivated by the second Korn's inequality, which holds for the RSI FEM discretization under consideration. This means that the estimate

$$\kappa(C_{DD}^{-1} K) = O((1-2\nu)^{-1})$$

holds uniformly with respect to the mesh size parameter in the FEM discretization. The first of the studied preconditioners is obtained by MIC(0) factorization of the blocks in (6).

3.1 Parallel MIC(0) preconditioning

The first method used is based on parallel MIC(0) preconditioner for scalar elliptic problems [3]. Its basic idea is to apply MIC(0) factorization of an approximation B of the stiffness matrix A. Matrix B has a special block structure. Its diagonal blocks are diagonal matrices. This allows the solution of the preconditioning system to be performed in parallel. The condition number estimate $\kappa(B^{-1}A) \leq 3$ holds uniformly with respect to mesh parameter and possible coefficient jumps (see for the related analysis in [3]). This technique is applied three times – once for each diagonal block of (6). Thus we obtain the parallel MIC(0) preconditioner in the form:

$$C_{DDMIC(0)} = \begin{bmatrix} C_{MIC(0)}(B) & & \\ & C_{MIC(0)}(B) & \\ & & C_{MIC(0)}(B) \end{bmatrix}.$$

More details on applying this preconditioner for the proposed homogenization technique can be found in [15].

3.2 BoomerAMG

Our second approach uses inner PCG iterations with BoomerAMG for A to approximate the DD block-diagonal matrix (6). BoomerAMG is parallel algebraic multigrid implementation, part of the software package HYPRE developed in Lawrence Livermore National Laboratory, USA. It can be used as a solver or as a preconditioner. Various different parallel coarsening techniques and relaxation schemes are available. See [14] for a detailed description of the coarsening algorithms, the interpolation and numerical results.

Version 2.0.0 of the Hypre library was used for the performed tests. Parallel modified independent sets (PMIS) coarsening was used in the presented tests. A V(1,1)-cycle with hybrid Gauss-Seidel smoothing is performed. The related AMG strength threshold is 0.5. Aggressive coarsening on the first two levels was utilized in order to decrease operator complexity. This noticeably reduced the memory footprint of the preconditioner. The number of inner iterations was fixed to 4.

4 Numerical Experiments

To solve the above described upscaling problem, a portable parallel FEM code was designed and implemented in C++. The parallelization has been facilitated using the MPI library [13].

The analyzed test specimens are parts of trabecular bone tissue extracted from a high resolution computer tomography image [7]. The voxel size is 37 μm. The trabecular bone has a strongly expressed heterogeneous microstructure composed of solid and fluid phases. To get a periodic RVE, the specimen is mirrored three times, see Fig. 1.

Homogenized properties of different RVEs with size of $n \times n \times n$, where $n \in \{32, 64, 128\}$, see Fig. 1. The Young modulus and the Poisson ratio of the solid phase, taken from [8], are $E^s = 14.7$GPa and $\nu^s = 0.325$. Our intention was to obtain the homogenized elasticity tensor of the RVE, taking into account the elastic response of the solid phase only. We interpret the fluid phase as a fictitious domain. On that account exponentially decreasing Young modulus $E^f = \zeta E^S$ for the voxels corresponding to the fluid phase are used, where ζ is the parameter decreased. We set $\nu^f = \nu^s$ which practically doesn't influence the numerical upscaling results.

The iteration stopping criterion was $||\mathbf{r}^j||_{C^{-1}}/||\mathbf{r}^0||_{C^{-1}} < 10^{-6}$, where $\mathbf{r}^j$ is the residual at the j-th iteration step of the preconditioned conjugate gradient method and C stands for the used preconditioner.

Numerical experiments were performed on a Blue Gene/P machine. It is a massively parallel computer consisting of quad-core nodes. The PowerPC based low power processors run at 850 MHz. Each node has 2GB of RAM. Nodes are interconnected with several specialized high speed networks—3D mesh network for peer to peer communications and tree network for collective communications, among others.

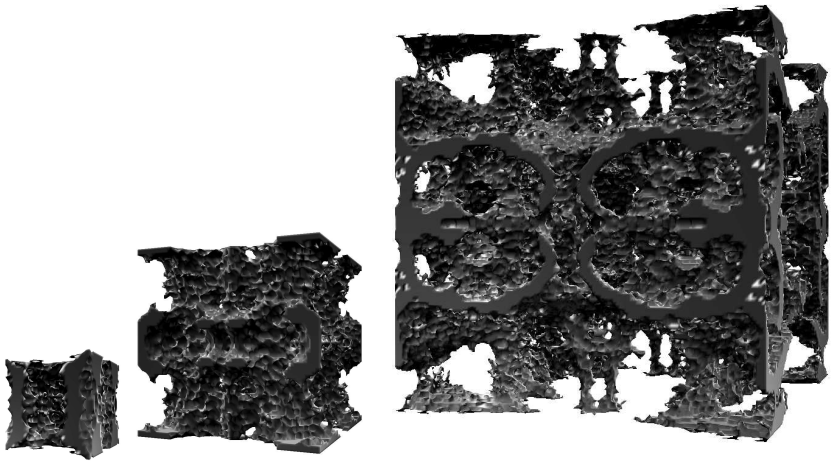

(a) (b) (c)

Fig. 1 Structure of the solid phase: (a) $n = 32$, (b) $n = 64$, (c) $n = 128$.

Starting on 2 processors for solution of the smallest problem ($n = 32$), the number of processors is increased proportionally to the number of unknowns, for the larger problems. In Table 1 are collected times T and number of iterations It for the MIC(0) preconditioner and for the solution of one subproblem (4). The results with the three RVEs and $\zeta \in \{10^{-1}, 10^{-2}, 10^{-3}, 10^{-4}, 10^{-5}\}$ are shown. The number of unknowns is indicated with N, and the number of processors – with p. The same information, but for BoomerAMG preconditioner is presented in Table 2.

Table 1 MIC(0)

			$\zeta = 10^{-1}$		$\zeta = 10^{-2}$		$\zeta = 10^{-3}$		$\zeta = 10^{-4}$		$\zeta = 10^{-5}$	
n	N	p	$T[s]$	It	$T[s]$	It	$T[s]$	It	$T[s]$	It	$T[s]$	It
32	2 396 160	2	267	219	455	378	689	576	816	684	836	701
64	19 021 824	16	442	320	804	588	1 235	907	1 683	1 239	1 937	1 426
128	151 584 768	128	937	462	1 715	851	2 939	1 462	3 953	1 969	4 634	2 309

Table 2 BoomerAMG

			$\zeta = 10^{-1}$		$\zeta = 10^{-2}$		$\zeta = 10^{-3}$		$\zeta = 10^{-4}$		$\zeta = 10^{-5}$	
n	N	p	$T[s]$	It	$T[s]$	It	$T[s]$	It	$T[s]$	It	$T[s]$	It
32	2 396 160	2	596	30	989	51	1 385	73	1 644	86	1 682	88
64	19 021 824	16	669	30	1 212	56	1 736	81	2 238	105	2 447	115
128	151 584 768	128	1 114	39	1 706	61	2 566	93	3 292	120	3 856	141

The number of iterations for both preconditioners increase gradually with the decrease of ζ. The available theoretical estimates for the convergence of the MIC(0) preconditioner concern some model problems for homogeneous materials. In such cases, the number of iterations is $n_{it} = O(n^{1/2}) = O(N^{1/6})$. Here the number of iterations has very similar behavior for $\zeta \in \{10^-1, 10^-2\}$. Nevertheless, even for very large coefficient jumps convergence is only slightly deteriorating. Slight increase in the number of iterations with the problem size is observed for the BoomerAMG preconditioner. We see similar parallel times for both MIC(0) and BoomerAMG preconditioners. BoomerAMG has some advantage for the largest problem in the case of strong coefficient jumps.

The obtained structure of the homogenized stiffness matrix C^H corresponds to the case of orthotropic materials in all of the experiments. This is due to the enforced triple mirroring procedure. Following (3), the Young moduli E_i in each of the coordinate directions and the Poisson ratios $\nu_{ij} = -\varepsilon_{jj}/\varepsilon_{ii}$ can be computed explicitly by the formulas

$$E_i = 1/s_{ii} \qquad \nu_{ij} = -E_i s_{ji}$$

where s_{ij} stand for the elements of the compliance matrix $S = (C^H)^{-1}$, see [5].

Tables 3, 4 and 5 contain the computed homogenized Young moduli, Poisson ratios and shear moduli for varying the fictitious domain Young modulus parameter ζ for the considered three different specimens.

Table 3 Homogenized material properties – $n = 32$

ζ	E_1	E_2	E_3	ν_{12}	ν_{23}	ν_{31}	μ_{23}	μ_{31}	μ_{12}
10^{-1}	4.52×10^9	6.23×10^9	6.24×10^9	0.208	0.300	0.286	2.29×10^9	1.39×10^9	1.35×10^9
10^{-2}	2.03×10^9	4.72×10^9	4.67×10^9	0.095	0.271	0.229	1.73×10^9	4.81×10^8	3.80×10^8
10^{-3}	1.67×10^9	4.48×10^9	4.45×10^9	0.074	0.264	0.212	1.66×10^9	3.56×10^8	2.42×10^8
10^{-4}	1.63×10^9	4.46×10^9	4.42×10^9	0.072	0.263	0.210	1.65×10^9	3.42×10^8	2.26×10^8
10^{-5}	1.62×10^9	4.45×10^9	4.42×10^9	0.071	0.262	0.210	1.65×10^9	3.40×10^8	2.24×10^8

Table 4 Homogenized material properties – $n = 64$

ζ	E_1	E_2	E_3	ν_{12}	ν_{23}	ν_{31}	μ_{23}	μ_{31}	μ_{12}
10^{-1}	2.86×10^9	3.11×10^9	3.55×10^9	0.288	0.270	0.281	1.19×10^9	9.07×10^8	9.50×10^8
10^{-2}	8.73×10^8	1.12×10^9	1.94×10^9	0.191	0.164	0.185	4.94×10^8	1.62×10^8	1.71×10^8
10^{-3}	5.69×10^8	8.02×10^8	1.73×10^9	0.127	0.124	0.117	3.90×10^8	5.22×10^7	5.22×10^7
10^{-4}	5.33×10^8	7.62×10^8	1.71×10^9	0.117	0.119	0.102	3.77×10^8	3.88×10^7	3.77×10^7
10^{-5}	5.29×10^8	7.58×10^8	1.71×10^9	0.116	0.118	0.101	3.76×10^8	3.74×10^7	3.62×10^7

A stable behavior of the implemented numerical homogenization scheme is observed in all cases. A good accuracy of the computed homogenized Young moduli and Poisson ratios is achieved if the fictitious domain modulus $E^f = \zeta E^s$ for $\zeta \in \{10^{-4}, 10^{-5}\}$. In all three cases the orthotropy ratio is about 3. This evidently

Table 5 Homogenized material properties – $n = 128$

ζ	E_1	E_2	E_3	ν_{12}	ν_{23}	ν_{31}	μ_{23}	μ_{31}	μ_{12}
10^{-1}	2.66×10^9	2.47×10^9	2.67×10^9	0.315	0.284	0.278	8.76×10^8	8.78×10^8	8.87×10^8
10^{-2}	7.90×10^8	5.97×10^8	9.51×10^8	0.282	0.180	0.171	1.93×10^8	1.68×10^8	1.64×10^8
10^{-3}	4.65×10^8	2.81×10^8	7.10×10^8	0.228	0.114	0.094	8.46×10^7	6.22×10^7	3.37×10^7
10^{-4}	4.20×10^8	2.24×10^8	6.78×10^8	0.222	0.100	0.076	6.66×10^7	4.89×10^7	1.40×10^7
10^{-5}	4.15×10^8	2.16×10^8	6.75×10^8	0.222	0.098	0.073	6.44×10^7	4.75×10^7	1.18×10^7

confirms that the hypothesis that the trabecular bone structure could be interpreted (approximated) as isotropic is not realistic.

Acknowledgements We gratefully acknowledge the support of the Bulgarian Supercomputing Center for the access to the IBM Blue Gene/P supercomputer. This work is partly supported by the Bulgarian NSF Grants DO02-115/08 and DO02- 147/08.

References

1. J. W. Ruge and K. Stüben. *Algebraic multigrid (AMG).* In S. F. McCormick, editor, Multigrid Methods, volume 3 of Frontiers in Applied Mathematics, SIAM, Philadelphia, PA, 1987, 73-130.
2. D. Malkus, T. Hughes. Mixed finite element methods. Reduced and selective integration techniques: an uniform concepts. *Comp. Meth. Appl. Mech. Eng.*,15: 63-81, 1978.
3. P. Arbenz, S. Margenov, and Y. Vutov, Parallel MIC(0) preconditioning of 3D elliptic problems discretized by Rannacher-Turek finite elements, *Computers and Mathematics with Applications*, **55** (10), 2008, 2197–2211.
4. D. N. Arnold and F. Brezzi, Mixed and nonconforming finite element methods: Implementation, postprocessing and error estimates, *RAIRO, Model. Math. Anal. Numer.*, **19**, 1985, 7–32.
5. M. H. Saad, Elasticity - Theory, Applications and Numerics, Elsevier, 2005.
6. O. Axelsson, *Iterative solution methods*, Cambridge University Press, Cambridge, 1994.
7. G. Beller, M. Burkhart, D. Felsenberg, W. Gowin, H.-C. Hege, B. Koller, S. Prohaska, P. I. Saparin, and J. S. Thomsen, Vertebral body data set esa29-99-l3, http://bone3d.zib.de/data/2005/ESA29-99-L3/.
8. S. Cowin, *Bone poroelasticity*, J. Biomechanics, **32** (1999), 217-238.
9. A. Bensoussan, J. L. Lions, and G. Papanicolaou, *Asymptotic analysis for periodic structures*, Elsevier, 1978.
10. R. H. W. Hoppe and S. I. Petrova, Optimal shape design in biomimetics based on homogenization and adaptivity, *Math. Comput. Simul.*, **65** (3), 2004, 257–272.
11. R. Blaheta, Displacement decomposition–incomplete factorization preconditioning techniques for linear elasticity problems, *Num. Lin. Alg. Appl.*, **1** (2), 1994, 107–128.
12. R. Rannacher and S. Turek, Simple nonconforming quadrilateral Stokes element, *Numer. Methods for Partial Differential Equations*, **8** (2), 1992, 97–112.
13. D. Walker and J. Dongarra, MPI: a standard Message Passing Interface, *Supercomputer*, **63**, 1996, 56–68.
14. V. E. Henson and U. M. Yang. *BoomerAMG: a parallel algebraic multigrid solver and preconditioner.* Applied Numerical Mathematics, 41(5), 2002,155-177. Also available as LLNL technical report UCRL-JC-141495.
15. S. Margenov and Y. Vutov, Parallel MIC(0) Preconditioning for Numerical Upscaling of Anisotropic Linear Elastic Materials, Lecture Nodes in Computer Science, to appear;